EXPERIMENTAL LINE PARAMETERS OF THE OXYGEN A-BAND AT 760 nanm

L. R. BROWN
Jet Propulsion Laboratory
California Institute of Technology
4800 Oak Grove Dr.
Pasadena, CA 91109, USA

and

C. PLYMATE

National Solar Observatory
Tucson, AZ

Manuscript papers	17
Figures	8
Tables	10

Running title: Oxygen A-band parameters

Send galley proofs to:

Dr. Linda R. Brown, MS 183-601, Jet Propulsion Laboratory
California Institute of Technology, 4800 Oak Grove Dr.,Pasadena, CA 91109, USA.
Phone: 818-354-2940 fax: 818-354-5148 email: linda@regina.jpl.nasa.gov

Key words: oxygen, line parameters, A-band, intensities, pressure broadening, calibration standards, high resolution spectroscopy

Abstract

To support atmospheric remote sensing applications, line positions, intensities, self- and nitrogen- broadened line widths and their temperature dependence and pressure-induced frequency shifts at room temperature were measured up to J' and N '= 22 for the oxygen A-band at 13122 cm^{-1}. Intensities were obtained with 1% precisions and 2% absolute accuracies using absorption spectra recorded at 0.02 cm^{-1} resolution with the McMath Fourier transform spectrometer (FTS) located at Kitt Peak National Observatory / National Solar Observatory in Arizona. The oxygen line positions were calibrated using near-infrared CO transitions as secondary frequency standards. The intensities and positions of seven H_2O lines near 13900 cm^{-1} were also remeasured to validate the FTS performance. The O_2 intensities fell within 1% of the values assumed for the molecular databases, but it was found that broadening coefficients and line positions should be revised for the A-band of molecular oxygen.

Key words: oxygen, A-band, line parameters, intensities, broadening coefficients, widths, pressure shifts, calibration standards

Introduction

The accuracies of the molecular parameters are a limiting factor in the determination of the atmospheric quantities like pressure and temperature from remote sensing spectra(1). The most important of these are the intensities. However, as seen in Table 1, the scatter among published intensity measurements for the A-band of O_2 (2-14) is significantly larger than the 1% accuracies required for current monitoring technologies; in fact, Table 1 omits several studies that reported more divergent values (see Refs. 9 and 13 and the references therein). Most of the band intensities in Table 1 fall into one of two groups. Some values (generally obtained through broadband integration) give an averaged value of 2.13×10^{-22} cm^{-2}/(molecule x cm^{-1}), while other band strengths (often reported from line-by-line analysis of high resolution spectra) result in a mean value of 2.28×10^{-22} cm^{-2} /(molecule x cm^{-1}). Values far from these two groups (2-4,14) are viewed as spurious.

For the 1996 version of the HITRAN database of molecular line parameters (15,16), the line intensities of the oxygen A-band at 760 nanm (13122 cm^{-1}) were revised using the work of Ritter and Wilkerson (12), even though their results were 8 - 10 % higher than band strengths available in the literature. The change represented an increase of 16% from the values assumed in earlier editions of HITRAN (17). This present study was undertaken at the end of 1997 primarily to validate the 1996 HITRAN intensities for EOS (Earth Observing Satellite) investigations like SAGE III (18) which desire 1% accuracies. Concurrently, independent studies of intensities and pressure broadening were performed by investigators using different spectrometers. Avetisov and Kauranen (7) measured two transitions using a two-tone frequency - modulation with diode lasers while Newnham et al. (9) used an Bruker FTS; these two studies supported a lower value of integrated intensity. More recently, Schermaul and Learner (13) obtained band strengths and self-broadened line widths at different temperatures from the measurement of some 65 individual transitions; their band strength fell close to the higher value of Ritter and Wilkerson. Finally, Looney et al. (11) measured one transition with a cavity ring-down spectrometer which matched the higher intensities. As will be described in this paper and shown in Table 1, our intensity measurements agreed with HITRAN values to within 0.2%, and

our self-broadened widths were within 2% those reported by Ritter and Wilkerson. We also measured nitrogen-broadened widths, pressure -induced frequency shifts and the temperature dependence coefficients for the widths. From these we computed corresponding air-broadened coefficients. Finally, we calibrated the O_2 line positions using the 2 - 0 and 3 - 0 bands of CO near 4260 and 6350 cm^{-1} (19,20) respectively. These form the basis for specific improvements in the database for the oxygen A-band.

Theoretical background

The A-band plotted in Fig. 1 arises from the (0 ← 0) vibration levels of the $b^1\Sigma^+_g$ - $X^3\Sigma^+_g$ electronic transition of molecular oxygen through its magnetic dipole moment (21). The rotational levels are described (22) by the angular momenta **N** and **J**, where J is total angular momentum equal to the sum of the rotational (N) and spin (S) angular momenta. The triply degenerate ground state $X^3\Sigma^+_g$ is comprised of levels designated by J" = N"-1, N", N"+1, with only odd values of N being allowed by symmetry. In the $b^1\Sigma^+_g$ upper state with S = 0, the only available states are those with even values of N and N = J. The A-band is then comprised of four types of transitions involving ΔN N"ΔJ J", limited to PP, PQ, RQ and RR. The expressions required to model the observed energies and the line intensities are essentially those given by Watson (22) and thoroughly described in previous studies (12,13,16,23-26).

For the HITRAN database (15), the ground state were obtained from the studies of Rouille et al. (23) and Zink et al. (24). The upper state levels of the A-band were computed from the analyses of Zare et al. (25) and Albritten et al. (26) using atmospheric and air-broadened laboratory data from the 1948 measurements by Babcock and Herzberg (21). As indicated earlier, the A-band intensities were taken from Ritter and Wilkerson (12). It was intended (as described in Table 3 of Gamache et al. (16)) that the air- and self- broadened widths for the A-band and the B-band also be based on the work of Ritter and Wilkerson (12) who had reported self-broadened widths and measured a few air-broadened lines. However, above 10000 cm^{-1}, all the oxygen widths from the 1992 HITRAN (17) were inadvertently retained; the older widths were higher by 5 to 15%. The temperature dependence of the widths in both databases was set to

0.71, and no pressure shifts were given. The present empirical measurements were undertaken in hopes of improving the 1996 HITRAN values.

Experimental details

Special care was taken in performing the experiment in order to obtain the best possible precisions and accuracies. Over three dozen laboratory absorption spectra were recorded at Doppler-limited (0.02 cm^{-1}) resolution using the FTS located at the National Solar Observatory on Kitt Peak Mountain in Arizona. These were obtained in four different sessions at Kitt Peak between October 1997 and March 1999. The optical source was a quartz projection lamp, the detectors were two matched Si photodiodes, and the beamsplitter was made of dynasil (fused silica) with a silver coating. The spectra were integrated for 70 to 80 minutes in order to achieve signal to noise ratios of 300 to 1 with a bandpass from 8700 to 15000 cm^{-1}; a sample spectrum is shown in Fig. 1.

The gas sample conditions are summarized in Table 2. The scans involving pure oxygen samples (set A) consisted of nine scans at room temperature and six at cold temperature (from 202 to 224 K) from which the intensities, self-broadening widths, temperature dependencies and pressure-induced frequency shifts at room temperature were obtained. The nitrogen-broadening coefficients were obtained from the runs labeled sets B and C in Table 2. The nitrogen-oxygen mixtures (set B) were made in the absorption chamber by adding increasing amounts of nitrogen for each successive scan. The resulting oxygen abundance ranged from 6% to 9%. Synthetic dry air (set C) from a cylinder was used for the six cold temperature scans. Ambient air at room temperature with 1% water (set D) was obtained by drawing air from the room into the absorption cell containing a few Torr of water; the partial pressure of oxygen was determined by subtracting the water pressure from the total and multiplying the resulting pressure by 0.2095 (27). Sets E and F were acquired to check of the FTS performance and to calibrate the oxygen line positions, respectively.

Three absorption cells were used. For most scans, a quartz single-pass cell 2.4 m long and a stainless-steel multi-pass (white) cell of 6-m-base were placed simultaneously in the optical

beam (as in Ref. 28). Then transitions in the $3\nu_3$ regions of H_2O at 10600 cm^{-1} (29) or C_2H_2 at 9600 cm^{-1} (30) were scanned simultaneously (with the oxygen samples) so that positions could be normalized to a common scale in order to determine the pressure shifts at room temperature. The footnote in Table 2 indicates which species were used for the calibration in specific scans. For the cold sample spectra, a coolable, stainless steel, 1-m-base multi-pass chamber was employed by itself. As a result, a consistent calibration was difficult to achieve from run to run so that the temperature dependence of the pressure shifts were not well determined. The external path between the cells and the FTS were purged vigorously with the effluent from two liquid nitrogen dewars. Empty cell scans were done to confirm that the purge was effective in removing absorptions of both water and oxygen arising from the atmosphere.

Pressures and temperatures were continually monitored during the scanning using capacitance manometers and thermistors (for the room temperature runs) or three platinum resistance thermocouples (imbedded in the barrel of the cold cell). When the 1000 Torr gauge was cross-calibrated against a mercury manometer, it read within 0.3% at 600 Torr. Temperatures were determined to 1.5 K for the room temperature scans and to 10 K for the cold data. The larger uncertainty for the cold data arose from fluctuations and temperature gradients across the length of the cell during the scanning and from some undetermined systematic problem with the thermocouples. Ultimately, for the cold scans, the rotational temperature of the gas was determined from the measured intensities. The effective temperatures were 5 - 7 K higher than the recorded values.

Experimental line parameters were retrieved from individual spectra using non-linear least squares curve fitting (31). As in Fig. 2, the differences between the observed and computed spectra are minimized by adjusting the values of the positions, intensities and widths. The measurements become the values used in the last iteration of the synthetic spectrum. A Voigt line shape computed using Humlicek (32,33) was sufficient for shorter path data because the optical depths were generally less than 50%. The exceptions were three long-path, room-temperature scans (listed with 25 m paths in Table 2) for which the optical depths were considerably larger. In these three, we observed a characteristic "w-shaped" residual of about1%

which was removed by using a Galatry (34) profile. The intensities retrieved from the longer path scans using the Galatry profile were within 0.5% of those obtained from the scans reduced with the Voigt line shape, but the Galatry widths were 1.5 to 2.5% higher than the Voigt widths.

When performing any empirical study, it is always wise to check the performance of the spectrometer by remeasuring known transitions. Unfortunately, in this spectral region there was a dearth of calibration standards for intensities (and also for frequencies (35)). However, a search of the literature revealed that the intensities of seven H_2O lines near 13900 cm^{-1} had been measured previously by four studies (36-39), and in addition, four H_2O spectra had already been recorded using the Kitt Peak FTS. In Table 3, the seven H_2O lines are shown with corresponding intensities obtained by averaging the individual values; the differences between the average and the values reported by each study are listed as well. To check the operation of the FTS during the present effort, five additional spectra of H_2O (set E in Table 2) were obtained during the sessions for the oxygen data using exactly the same resolution, detectors, cells, pressure gauges and optical alignments. These data confirmed that the FTS had a good zero for totally saturated features and that, as seen in Table 4, the retrieved line intensities of the standard H_2O lines could be reproduced to within 1.4% ($\pm$ 0.9%) of the averaged values. Two additional low pressure spectra of CO were also obtained (not listed in Table 2). The 3 - 0 band intensities retrieved from these spectra agreed within 2.0% of the independent measurements by Henningsen et al. (40), Picque et al. (41); the intensities from the CO spectra are being combined with the new data recorded with a Bomem and reported separately (42).

To calibrate the oxygen A-band line positions, a broad band spectrum covering the 3800 to 15000 cm^{-1} region was also obtained to reference the O_2 line positions to the positions of the 2 - 0 and 3 - 0 bands of CO (19,20). For this run, a Si-photodiode and an InSb detector were used simultaneously, in the manner done previously with the Kitt Peak FTS by Mandin et al. (36). The sample conditions involving a mixture of water, carbon monoxide and oxygen in the long path cell and acetylene in the 2.4 m cell are listed in Table 2 (set F). Some two dozen transitions of the 2 - 0 band of CO from 4294 to 4336 cm^{-1} and 33 transitions of the 3 - 0 band of CO from 6270 to 6400 cm^{-1} were matched to the reported values of Pollock et al. (19) and Picque and

Guelachvilli (20) respectively to determine the multiplying correction factor of 1.0000000018 [33] for the observed positions. The rms agreement for the calibrated lines in the two CO bands was 0.00018 cm^{-1}, and the difference between the calibrated and "raw" O_2 positions was only 0.00025 cm^{-1}. The uncertainty for the calibration factor implied that the absolute accuracy of the oxygen positions above 10000 cm^{-1} was 0.001 cm^{-1} at best. This is somewhat verified by the comparison of water positions shown in Table 4 using lines previously calibrated by Mandin et al. (36) using the same FTS and lines of N_2O previously referenced to 2 - 0 band of CO (19). Therefore, the precisions of the positions seem to be at least ± 0.0003 cm^{-1}, and the absolute accuracies are thought to be 0.0015 cm^{-1} or better.

Satisfied with these checks of the instrument, we then proceeded with the systematic reduction of the data. Spectra involving the pure oxygen were used to obtain the intensities along with the self-broadened widths (γ= HWHM) and pressure-induced frequency shifts ($\delta = \nu(\text{shifted}) - \nu_o$). The room and cold temperature widths of each transition were combined to determine the temperature dependence coefficient "n" from $\gamma / \gamma_o = [T_o / T]^n$ for each upper state J,N. The pure oxygen Lorentz widths from set A data were fitted to the linear expression $\ln [\gamma] = \ln [\gamma_o] + n \ln [T_o / T]$. For the cold scans, the effective temperature T was the rotational temperature of the gas obtained from the measured intensities. T_o was set to 296. K so that a least-squared fitted width at 296 K could be obtained from the intercept $\ln [\gamma_o]$, The $[\gamma_o]$ widths from the cold and warm data combined were generally within 1% of the widths obtained from the room temperature data alone. For the pressure shifts, the observed line positions from the various scans, including low pressure spectrum from the set F, were calibrated using water or acetylene transitions, and a linear fit of shift vs pressure was performed for each transition. For the retrieval of the nitrogen-broadening coefficients, the self -broadened line widths and shifts of the present experimental results were used to remove the self-broadened contribution from the total observed total width and shift in order to compute the N_2 - contribution. The pressure shifts obtained from the moist air spectra (set D) were found to be in general agreement with the observed shifts from data sets A and B.

Although not used for the final determination of intensity shown in the next section, the

derived A-band intensity obtained from the nitrogen-oxygen mixtures and moist ambient air were also considered. In Table 5, the observed / calculated intensity ratios are given for four data sets; the calculated intensities are taken from the 1996 HITRAN database (15). The number in parentheses is the rms in percent for some 44 measured lines. The three sets (A,B and D in Table 2) involving pure oxygen, mixed nitrogen with oxygen and moist ambient air agree with an rms of 0.5% (± 1.%). One very surprising result is that the intensities from a few additional spectra using commercial dry air at room temperature (labelled dry air in Table 5) produced intensities that were 10.5% lower. An oxygen abundance of 20.95% was assumed for both the " synthetic dry air" and "moist room air, and yet the A-band intensities obtained were very different. Because of this discrepancy, the room temperature dry air runs are not listed in Table 2, and they were used only to determine the actual abundance of oxygen (18.7%) in the cold sample scans (set C). The cylinder of dry air had been purchased three or four years early; perhaps some oxidation had occurred changing the partial pressure of oxygen. This is not the first instance in which synthetic dry air from a cylinder contained less oxygen than natural atmospheric air; Liebe et al. (43) noted a 2.5% oxygen deficit with a cylinder of synthetic dry air. One of course immediately wonders if this variation in air sample could have contributed to the variation of intensity results for the A- band, but in fact very few investigators (9) have used synthetic dry air for the intensity measurements.

In a sense, we have performed the intensity portion of the experiment three times using three different types of gas samples (pure oxygen, oxygen plus nitrogen mixed in the cell and moist ambient air), and the observed intensities from the three sets agree within 0.5% ±1.%. Our experimental intensities of seven H_2O line and some 30 CO transitions are within 1.5% to 2% of with reported values in the literature. These comparisons thus lead us to believe that our absolute accuracies for intensities are 2.0% or better for the A-band of oxygen. The precisions and accuracies of the positions, widths and shifts are evaluated in the next section.

Results and Discussion

The individual measurements for 44 transitions of the oxygen A-band listed in Table 6 are

grouped according to the upper state quantum number J' = N.' The observed positions and intensities in natural abundance (without correcting for the isotopic abundance) are shown along with the corresponding %rms and the upper state value of J (= N). The intensities are taken from set A spectra. These are followed by the self- and nitrogen- pressure broadened coefficients: the line widths (HWHM) and frequency-induced pressure shifts. The last entry is the quantum assignment showing ΔN N"ΔJ J". The experimental uncertainties (computed as the percent rms agreement between measurements from different spectra) are shown in parentheses. The units are, respectively, wavenumbers (cm^{-1}) for the positions, cm^{-2}/atm at 296 K for the intensities in natural abundance, and cm^{-1}/atm at 296 K for the widths and shifts.

The intensities are considered first. The experimental precisions are confirmed to be ±1% by comparing experimental and calculated values in Fig. 3. For this comparison, the calculated intensities in normal isotopic abundance are taken directly from the 1996 HITRAN database (15) which had adopted (16) the intensities of Ritter and Wilkerson (12). The mean differences between the 44 observed and calculated intensities are -0.2% with an rms or 1%, thus confirming the HITRAN calculated intensities and the Ritter and Wilkerson measurements. As was seen in Table 1, the present values fall within 1% of results reported by Ritter and Wilkerson (who used a diode laser spectrometer) and Schermaul and Learner (13) (who used a Bruker FTS). Moreover, with a cavity ring-down spectrometer, Looney et al. (11) obtained a intensity of the PQ (9) which implied a band strength 1.4% lower than Ritter and Wilkerson. In contrast, the two transitions of Avetisov and Kautanen (7) and the integrated intensity of Newnham et al. (9) (who also used the same Bruker FTS as Schermaul and Learner) are both closer to the lower set of band intensities (most of which were determined by integrating the whole spectrum). Like Ritter and Wilkerson, we do not observe the Herman-Wallis factor reported by Schermaul and Learner, however. There is no clear explanation why lower resolution studies obtain lower values of band strengths compared to most of the high resolution studies that measure individual lines (with the exception of Avetisov and Kautanen (7)). We do note that the absolute accuracy of the measurements in the earlier decades are estimated to be 4 to 8%, and this contributes to part of the differences. However, given the number of attempts to measure the intensities, it is

surprising that the global average of measured band strengths do not match recent high accuracy determinations. In any case, given the exceptional agreement of present results with the HITRAN calculation and with three line-by-line studies (11-13) which used different types of spectrometers, no further analysis for band strength and dipole moments was performed in the present study. The present study indicates that no changes should be made in the HITRAN database for the oxygen A-band intensities at this time.

The pressure broadening coefficients listed in Table 6 are interesting in themselves. As seen in Figs. 4 and 5, where the self- and nitrogen-broadened widths are plotted as a function of the upper state J = N, these coefficients vary smoothly according to the upper state quanta. The difference of widths at the highest J indicates a breakdown of the experimental precision, but the observed widths of the low N=J lines, particularly R1R1, are thought to be representative of their true behavior rather than poor measurement. The experimental precisions of the widths of ±1.5% or better (based on the %rms agreement between spectra) are easily validated because, as seen in Table 6 and Figs. 4 and 5, the oxygen A-band transitions to the same upper state energy level have the same widths. This behavior is in contrast to the widths of other diatomic molecules like HF (44) or NO (45) for which transitions of the same "m" have similar widths (where m is J" for P branch lines and J"+1 for R branch lines); for example, the widths of P3 and R2 are nearly equal in HF and NO. For each A-band transition of oxygen, the self- and N_2- broadened widths are also nearly equal, as seen in Table 6. The self-broadened widths are slightly smaller at low J and become slightly larger than the N_2- broadened widths near J' = 14. This is consistent with the observations of Ritter and Wilkerson who measured seven air-broadened widths and reported the ratio of air-/self- broadened widths to vary from 1.025 at J' = 0 to 1.002 at J' = 20.

Because the widths vary in this manner as a function of the upper state quantum numbers, widths for the four transitions associated with the same upper state can be averaged together to achieve better precision (but not absolute accuracy); these are shown in Table 7. In the middle columns are shown the averaged widths, the experimental uncertainty (%rms based on the average of four values) and also an observed - calculated widths in percent; the calculated widths are obtained by fitting the observed widths to quadratic expressions given in the lower half of

Table 7. The rms of the observed minus calculated widths is 1.2% and 1.1% for the self- and nitrogen-broadened widths, respectively, confirming an experimental precision based on agreement between individual spectra. In the last column of Table 7, the air-broadened widths are computed from the averaged observed self- and N_2 - broadened widths assuming a "natural air" with 20.95% oxygen and the remainder assumed to be nitrogen (thus ignoring the 0.9% argon abundance).

While there have been numerous studies in which a few selected line widths of oxygen were measured (such as 46-50 and the references therein), only the two studies of the A-band which measured self-broadening through the whole band at high resolution (12,13) are being considered for detailed comparison. Both Ritter and Wilkerson and Schermaul and Learner give plots of self-broadened widths vs quantum numbers for a number of other studies; since the present self-broadened results overlay the Wilkerson and Ritter values so closely, the reader is referred to these papers. Instead, the J,N-averaged self-broadened widths of the present study from Table 7 are compared to the corresponding J,N-averaged values computed from Refs. 12 and 13. For this, the ratios of the J-averaged widths of the other studies to the present values are plotted in Fig. 6 as a function of J'. The Ritter and Wilkerson study is only 2% higher than the present study, but the Schermaul and Learner values are 11 to 15% higher. It is important to note that the present FTS data were reduced assuming a Voigt shape for the higher pressure data, whereas the Ritter and Wilkerson study modelled their diode laser spectra with a Galatry profile. Schermaul and Learner (13) did not have a Galatry profile implemented, so they instead used the Voigt expressions and decreased the effective oxygen Doppler width based on the Galatry narrowing coefficient. As a result, their widths are in a sense a "non-standard" result. Therefore it would not be appropriate to attempt to obtain more precise and accurate line widths by simply taking averages of widths of Ritter and Wilkerson, the Schermaul and Learner and the present study. Attention must be given to what line shape will be used in a given application. To facilitate the computation of the Lorentz widths, the polynomials at the bottom Table 7 are recommended for applications that assume a Voigt profile. The comparison in Fig. 6 suggests that corresponding Galatry widths may be obtained by a +2% scaling of these computed Lorentz

widths. It is thought that the present widths have an overall precision of 1.2% and an absolute accuracy of 2.5%.

The widths at cold temperatures displayed similar variation with J' = N'. Therefore, the fitted temperature dependence coefficients of four individual transitions involving the same upper state levels were averaged together to obtain the values listed in Table 7. The temperature coefficients decrease with increasing J', N', going from a high of 0.77 to 0.6; The % uncertainty in parenthesis is the rms agreement between the "n" values for the four individual transitions; this rms should be taken as an upper limit for precision since the precisions for the individual transitions are generally no better than 10%. Since the self- and nitrogen-broadened temperature dependences are so similar, we reason that more precise values can be obtained by averaging these two coefficients at each J', and we recommend these averages (shown in the last column of Table 7) be used for air-broadening temperature dependences in the databases. Based on the width uncertainties and the gas temperature uncertainties, the absolute accuracies of the temperature coefficients are estimated to be only ±15%. A large error source in the determination of these coefficients is that fact that the rotational temperatures of the gas based on the line intensities was some 6 K higher than the temperatures indicated by the thermocouples. Despite these large uncertainties, the present values do compare well with the average temperature dependence coefficient of 0.69 reported by Schermaul and Learner (13) for self-broadened widths and the value of 0.71 assumed in the 1996 HITRAN database (15,16) for air-broadened widths; as shown in Table 7, the average of all present computed air-broadened temperature dependence coefficients is 0.70.

The line positions listed in Table 6 are determined from a spectrum recorded with two absorption cells containing mixtures of CO, O_2, H_2O and C_2H_2 at low pressure (set F in Table 2). The set of empirical upper state energies in Table 7 are obtained by adding the calculated from state from the 1996 HITRAN to the four transitions involving the same upper state level. The rms agreement of the energies levels shown in parentheses indicates the line center precisions to be 0.00035 cm^{-1}. Unfortunately, the absolute accuracy of the calibration can not be confirmed because the reported positions in the literature differ greatly (by a much as a factor

of 30 compared to our precision). As seen in Table 8, the present positions are 0.0015 (± 0.0007) cm^{-1} higher than the "uncalibrated" positions given by Schermaul and Learner (13) who relied on the internal calibration of the Bruker FTS. They are also higher by 0.0030 (± 0.0070) cm^{-1} than the values of Kanamori et al. (51). Moreover, our positions are systematically higher by 0.0120 cm^{-1} (± 0.0005) cm^{-1} from those recently reported by Phillips et al. (52) who used Argon and Iodine transitions as standards. Because of this wide variation, a numerical check of the present results was done by Brault (53) who performed peak-finding on the same calibration spectrum using different software; the positions were the same within 0.0002 cm^{-1}. They also agreed to within 0.0002 cm^{-1} with unpublished values obtained by Brault (53) using other spectra recorded in the 1980's with the same FTS and calibrated with N_2O lines references to the 2 - 0 band of CO. Thus the present positions are consistently reproduced from different data sets recorded with the Kitt Peak FTS over a period of almost two decades.

The discrepancy in absolute accuracy for the line positions warrants further investigation by other groups to resolve this. The available standards (35) for the visible wavelengths seem to have uncertainties of 0.002 cm^{-1} and worse. Individuals who use the water lines (29,36) are expected to be systematically off by from those who chose Phillips et al. (54) oxygen positions as the calibration standards. Several studies have already measured the A-band positions to precisions of 0.0007 cm^{-1} or better (and in fact the unpublished data of Brault appear to have precisions of better than 0.0001 cm^{-1} so that a new fit of the ground state may be needed). If the absolute positions and self-broadened pressure-induced frequency shifts could be validated, the A-band of oxygen would be a convenient calibration standard for the visible region. However, because of these current discrepancies, detailed analysis of the positions is being deferred until new investigations can be attempted.

The high resolution studies (present, Schermaul and Learner and the Phillips et al.)) show that the positions being used in the HITRAN database (15,17) have systematic differences that change with quantum number. For example, in Table 8 the differences between the present positions and 1996 HITRAN values vary from 0.0128 cm^{-1} at low J to 0.0046 cm^{-1} at J = 20. This is partly because HITRAN A-band positions are based on old line data (21) in which the

line centers were pressure-shifted; the "gas sample" of Babcock and Herzberg was an open air path of 30 m, and their calibration standards were Ne lines. The old rotational constants for the upper state levels have in a sense absorbed the effects of the pressure shifts, and better values of B and D are now available from the work of Phillips et al. (54). However, before the line positions can be revised in the databases, the band center must be validated.

For atmospheric remote sensing, the air-broadened shifts must also be known. In principle, the values in Table 6 provide the necessary information for shifts. Like the widths and temperature coefficients, the present self- and nitrogen-broadened shifts often have similar values for each transition. Therefore the precisions of the air-broadened pressure shifts can be improved by simply averaging the measured self- and N_2-shifts; these have been listed in Table 6 in the column labelled "average." Unfortunately, other reported laboratory measurements of shifts in the literature (54-59) are scarce or are inconsistent with the present results. As seen in Table 9, the self-broadened shifts of two transitions reported by Avetisov and Kauranen (7) are similar to the present values: for R15Q16 -0.00575 (10) vs the present -0.0053 (3) cm^{-1}/atm and for R17R17 -0.00610 (15) vs the present -0.0051 (7) cm^{-1}/atm. Older studies (55-59) for self- and air-broadened shifts also reported averaged shifts between - 0.004 and -0.008 cm^{-1}/atm. However, the present results do not agree with a recent study by Phillips and Hamilton (54) who measured the most individual transitions. As indicated in Table 9, unlike the present study, their self- and nitrogen-broadened shifts are not nearly equal, and the size of the shifts are much larger than the present values; their self-broadened shifts range from - 0.007 to -0.017 cm^{-1}/atm while their nitrogen-broadened shifts range from 0.016 to -0.021 cm^{-1}/atm.

The lack of validation from other experiments and the scatter within the absolute calibration of the positions therefore cause some concern about the absolute values of the pressure-induced frequency shifts listed in Table 6. The wavenumber scales for the oxygen spectra at 13122 cm^{-1} have been normalized using C_2H_2 at 9600 cm^{-1} and H_2O at 10600 cm^{-1} and perhaps there may be systematic errors arising because the lines of the two species are 2500 to 3500 cm^{-1} apart. The absolute accuracy of the shifts is therefore taken to be no better than $\pm$ 0.0015 cm^{-1} /atm (even when the computed precisions shown in Table 6 are a factor of 5 smaller). However, if

one assumes that the widths are at least internally consistent, then the plots of self- and nitrogen-broadened shifts in Figs. 7 and 8, respectively, highlight some interesting trends vs the upper state J = N. Both set of shifts are negative and become increasingly more negative with increasing upper state J. For the N_2- broadened shifts, the PP and PQ type transitions are generally larger than the corresponding RQ and RR type at each J' up to J = 15; a similar pattern is barely discernible in the self- broadened shifts. Therefore, unlike the widths, the shifts for lines to the same upper state levels at not exactly the same at each J' and N'. Additional effort is needed to obtain a consensus about the shifts, and this will require full and careful measurement across the whole band.

The precisions and absolute accuracies of the five types of empirical parameters being reported have been carefully evaluated here. Our estimates for these uncertainties are summarized in Table 10.

Conclusion

Atmospheric applications require that the transition parameters be known with confidence, and this can be achieved only by several investigators repeating important measurements using different spectrometers. In the present study, the line intensities of the oxygen A-band at 13122 cm^{-1} have been measured with precisions of 1% and absolute accuracies of 2%. The accuracies are confirmed by comparing our measurements for oxygen, water and carbon monoxide with those of other investigators who used diode laser, Fourier transform and cavity ring-down spectrometers. The present measurements and those of three other studies are within 1% of the A-band intensities currently being used in the 1996 HITRAN database. However, there remains a puzzling mystery in that intensities generally measured from broadband integration of the spectrum are 7% lower than most of the recent line-by-line analysis. Some of the discrepancies with older measurements are likely due to their experimental uncertainties (4 to 8%). Pressure broadening coefficients (self- and nitrogen- broadened widths, temperature dependencies and shifts) are now available for atmospheric applications, and these should be incorporated into the next edition of the database. Within the precisions of the present data, the broadening

coefficients are seen to vary smoothly with the upper state quanta, and for each transition in the A-band, the self- and nitrogen-broadening coefficients are nearly equal.

It is surprising that line parameters of a simple molecule like oxygen have remained so uncertain for so long. Its investigators have been challenged to obtain absolute accuracies commiserate with their demonstrated precisions. We hope that the results reported here will be confirmed by other studies to remedy this situation. The oxygen A-band will be very useful as a laboratory calibration standard at the visible wavelengths if the line positions and pressure-induced frequency shifts can be validated and improved.

Acknowledgements

The authors wish to thank J. Brault, R. Schermaul and J. Looney for generously sharing information about the oxygen A-band in advance of publication. Part of the research described in this paper was carried out by the Jet Propulsion Laboratory, California Institute of Technology, under contract with the National Aeronautics and Space Administration.

References

1. D. M. O'Brien, S. A. English, and G. DaCosta, *J. Appl. Meteorology* **14**, 105-119 (1997).

2. V. D. Galkin, L. N. Jukove, and L. A. Mitrofanova, *Opt. Spectrosc.* **33**, 837-843 (1972).

3. B. E. Grosssman, C. Cahen, J. L. Lesne, J. Bernard, and G. Leboudec, *Appl. Opt.* **25**, 4261-4267 (1986).

4. J. H. Miller, R. W. Boese, and L. P. Giver, *J. Quant. Spectrosc. Rad. Transfer* **8,** 1507-1517 (1969).

5. L. Wallace and D. M. Hunten, *J. Geophys. Res.* **73**, 4813-4834 (1968).

6. T. G. Adiks and V. I. Dianov-Klokov, *Izv. Akad. Nauk. SSSR Fiz.Atmos. Okeana.* **4,** 605 - 609 (1968).

7. V. G. Avetisov and P. Kauranen, *Appl. Opt.* **36**, 1043-1054 (1997).

8. C. W. Cho, E. J. Allin, and H. L. Welsh, *Canad. J. Phys.* **41,** 1991-2002 (1963).

9. D. A. Newnham and J. Ballard, *J. Geophys. Res.* **103**, 28801-28816 (1998).

10. D. E. Burch and D. A. Gryvnak, *Appl. Opt.* **8**, 1493-1499 (1969).

11. J. P. Looney, R. D. vanZee, and J. T. Hodges, *Appl. Opt.* (in press).

12. K. J. Ritter and T. D. Wilkerson, *J. Mol. Spectrosc.* **121**, 1-19 (1987).

13. R. Schermaul and R. C. M. Learner, *J. Quant. Spectrosc. Rad. Transfer* **61**, 781-794 (1999).

14. G. D. Greenblatt, J. J. Orlando, J. B. Burkholder, and A. R. Ravishankara, *J. Geophysc. Res.* **95**, 18577-18582 (1990).

15. L. S. Rothman, C. P. Rinsland, A. Goldman, S. T. Massie, D. P. Edwards, J.-M. Flaud, A. Perrin, C. Camy-Peyret, V. Dana, J. Y-. Mandin, J. Schroeder, A. McCann, R. R. Gamache, R. B. Wattson, K. Yoshino, K. V. Chance, K. W. Jucks, L. R. Brown, V. Nemtchinov, and P. Varanasi, *J. Quant. Spectrosc. Rad. Transfer* **60**, 665-710 (1998).

16. R. R. Gamache, A. Goldman, and L. S. Rothman, *J. Quant. Spectrosc. Rad. Transfer* **59,** 495-509 (1998).

17. L. S. Rothman, R. R. Gamache, R. H. Tipping, C. P. Rinsland, M. A. H. Smith, D. C. Benner, V. Malathy Devi, J.-M. Flaud, C. Camy-Peyret, A. Perrin, A. Goldman, S. T. Massie, L. R. Brown, and R. A. Toth,. *J. Quant. Spectrosc. Rad. Transfer* **48**, 469-507 (1992).

18. P. H. Wang, G. S. Kent, M. P. McCormick, L. W. Thomason, and G. K. Yue, *Appl. Opt.*

35, 433-440 (1996).

19. C. R. Pollock, F. R. Petersen, D. A. Jennings, J. S. Wells, and A. G. Maki, *J. Mol. Spectrosc.* **99**, 357-368 (1983).

20. N. Picque and G. Guelachvili, *J. Mol. Spectrosc.* **185**, 244-248 (1997).

21. H. D. Babcock and L. Herzberg, *Astrophys. J.* **108**, 167-190 (1948).

22. J. K. G. Watson, *Canad. J. Phys.* **46**, 1637-1643 (1968).

23. G. Rouille, G. Millot, R. Saint-Loup, and H. Berger, *J. Mol. Spectrosc.* **154**, 372-382 (1992).

24. L. R. Zink and M. Mizushima, *J. Mol. Spectrosc.* **125**, 154-158 (1987).

25. R. N. Zare, A. L. Schmeltekopf, W. J. Harrop, and D. L. Albritton, *J. Mol. Spectrosc.* 46, 37-66 (1973).

26. D. L. Albritton, W. J. Harrop, and A. L. Schmeltekopf, *J. Mol. Spectrosc.* **46**, 103-118 (1973).

27. W. Baker and A. L. Mossman, Matheson Gas Data Book, sixth edition, pp 11, Secaucus, NJ, 1980.

28. L. R. Brown and R. A. Toth, *J. Opt. Soc. Am. B* **2**, 842-856 (1985).

29. J. P. Chevillard, J.-Y. Mandin, J.-M. Flaud, and C. Camy-Peyret, *Can. J. Phys.* **67**, 1065-1084 (1989).

30. M. Herman, T. R. Huet, and M. Vervloet, *Mol. Phys.* **66**, 333-353 (1989).

31. L. R. Brown, J. S. Margolis, R. H. Norton, and B. Stedry, *Appl. Spectrosc.* **37**, 287-292 (1983).

32. J. Humlicek, *J. Quant. Spectrosc. Rad. Transfer* **21**, 309-313 (1979).

33. J. Humlicek, *J. Quant. Spectrosc. Rad. Transfer* **27**, 417-444 (1982).

34. P. L. Varghesse and R. K. Hanson, *Appl. Opt.* **23**, 2376-2385 (1984).

35. G. Guelachvili, M. Birk, C. J. Borde, J. W. Brault, L. R. Brown, B. Carli, A. R. H. Cole, K. M. Evenson, A. Fayt, D. Hausamann, J. W. C. Johns, J. Kauppinen, Q. Kou, A. G. Maki, K. N. Rao, R. A. Toth, W. Urban, A. Valentin, J. Verges, G. Wagner, M. H. Wappelhorst, J. S. Wells, B. P. Winnewisser, and M. Winnewisser, *Pure and Appl. Chem.* **68**, 193-208 (1996).

36. J. Y. Mandin, J. P. Chevillard, C. Camy-Peyret, J. M. Flaud, and J. W. Brault, *J. Mol. Spectrosc.* **116**, 167-190 (1986).

37. T. D. Wilkerson, G. Schwemmer, B. Gentry, and L. P. Giver, *J. Quant. Spectrosc. Rad. Transfer* **22**, 315-331 (1979).

38. B. E. Grossmann, and E. V. Browell, *J. Mol. Spectrosc.* **136**, 264-294 (1989).

39. K. Singh and J. J. Obrien, *J. Mol. Spectrosc.* **167**, 99-108 (1994).

40. J. Henningsen, H. Simonsen, T. Mogelberg, and E. Trudso, *J. Mol. Spectrosc.* **193**, 254-362 (1999).

41. N. Picque, G. Guelachvili, V. Dana, and J.-Y. Mandin, *J. Mol. Struct.* (submitted).

42. C. Chackerian Jr., L. Giver, L. R. Brown, and R. Kshirsagar (in preparation for *J. Mol. Spectrosc.*)

43. H. J. Liebe, P. W. Rosenkranz, and G. A. Hufford, *J. Quant. Spectrosc. & Rad. Transfer* **48**, 629-643 (1992).

44. A. S. Pine and J. P. Looney, *J. Mol. Spectrosc.* **122**, 41-55 (1987).

45. C. Chackerian, Jr. R. S. Freedman, L. P. Giver, and L. R. Brown, *J. Mol. Spectrosc.* **192**, 215-219 (1998).

46. B. Ray, D. Biswas, and P. N. Ghosh, *J. Mol. Struct.* **407**, 39-46 (1997).

47. B. Ray and P. N. Ghosh, *Spectrochimia Acta A* **53**, 537-543 (1997).

48. A. Lucchesini, M. Derosa, C. Gabbanini, and S. Gozzini, *Nuov. Cim. D.* **20**, 253-260 (1998).

49. N. Seiser and D. C. Robie, *Chem. Phys. Lett.* **282**, 263-267 (1998).

50. D. A. Jennings, K. M. Evenson, and M. D. Vanek, *Geophys. Res. Lett.* **14**, 722-725 (1987).

51. H. Kanamori, M. Monona, and K. Sakurai, *Canad. J. Phys.* **68**, 313-316 (1990).

52. A. J. Phillips, F. Peters, and P. A. Hamilton, *J. Mol. Spectrosc.* **184**, 162-166 (1997).

53. J. W. Brault (private communication).

54. A. J. Phillips and P. A. Hamilton, *J. Mol. Spectrosc.* **174**, 587-594 (1995).

55. T. G. Adikis and V. I. Dianov-Klokov, *Opt. Spectrosc.* **30**, 110-111 (1971).

56. T. G. Adikis and V. I. Dianov-Klokov, *Opt. Spectrosc.* **32**, 226-228 (1972).

57. V. D. Galkin, *Opt. Spectrosc.* **35**, 367-369 (1973).

58. V. D. Galkin, *Opt. Spectrosc.* ***46***, 106-107 (1979).

special characters

† footnote

‡ footnote

μ small Greek mu

δ small Greek delta

γ small Greek gamma

Δ Large Greek delta

ν small Greek nu

$b^1\Sigma^+_g$ Please insert overstrike on the ^+_g

List of Tables

Table 1 Comparison of Band Strengths of the Oxygen A-band at 13122 cm^{-1} (760 nanm)†

Ref. #	Study	#Lines Meas.	Instrument or Retrieval type	Band Strength x 10^{-22} $cm^{-1}/(molecule \cdot cm^2)$
2.	Galkin et al. (1972)		Integrated low resolution	1.87
3.	Grossman et al. (1986)	6	Diode laser	1.97 (2)
4.	Miller et al. (1969)		Integrated low resolution	1.98
5.	Wallace / Hunten (1968)		Integrated low resolution	2.11
6.	Adiks / Dianov-Klokov (1968)		Integrated low resolution	2.11
7.	Avetisov / Kauranen (1997)	2	TTFMS, laser	2.11 (1)
8.	Cho et al. (1963)		Integrated low resolution	2.14
9.	Newnham / Ballard (1998)		FTS Integrated	2.143 (13)
10.	Burch / Gryvnak (1967)		Integrated low resolution	2.18
11.	Looney (in press)	1	Cavity ring-down (implies)	2.25
**	Present Study	44	FTS	2.28 (4)
12.	Ritter/Wilkerson (1986)	50	Diode laser	2.28 (4)
13.	Schermaul (in press)	65	FTS	2.30 (1)
14.	Greenblatt et al. (1990)			3.1 (3)
15.	Assumed for 1996 HITRAN (using Ritter/ Wilkerson)			2.28

Averaged Band Intensity

Using all but Ref. 14 :	2.13 ± 6%
Using Refs. 5 - 10:	2.13 ± 1.3%
Using Refs. 11 -13 and the present study:	2.28 ± 0.9%.

† FTS is Fourier transform spectrometer, and TTFMS is two-tone frequency-modulation spectroscopy with diode lasers.
The older low resolution measurements are assumed to have absolute accuracies of 4 to 8%.
The values in parentheses are the precisions quoted by the authors.

Table 2 EXPERIMENTAL CONDITIONS OF KITT PEAK FTS SPECTRA

Path m	O_2 Pres Torr	Temp K		Path m	O_2 Pres Torr	Temp K	N_2 Pres Torr	
A)	PURE OXYGEN			B)	NITROGEN + OXYGEN			
2.40	596.3	295.5	a	289.0	36.0	296.3	557.0	b
2.40	554.8	296.7	a	145.0	36.0	296.7	522.9	b
2.40	508.7	296.7	a	73.0	36.0	296.8	503.6	b
8.28	495.4	294.0		73.0	35.9	296.9	451.0	b
2.40	441.7	297.2	a	73.0	36.0	296.9	403.5	b
2.40	388.4	297.1	a	73.0	35.9	296.7	355.0	b
25.0	249.9	292.5	b					
25.0	197.5	292.7	b					
25.0	147.5	292.9	b	C)	DRY AIR (from cylinder)			
8.28	574.4	221.0		16.3	115.2	212.5	478.0	
8.28	516.0	224.0		16.3	111.2	217.2	462.0	
8.28	508.0	219.0		16.3	105.8	208.5	439.7	
16.3	449.0	205.0		16.3	101.3	213.5	421.0	
8.28	401.3	224.0		16.3	96.8	207.5	402.0	
16.3	318.0	203.0		16.3	87.8	211.0	364.6	
E)	PURE WATER			D)	MOIST AIR (ambient)			
97.0	5.02	291.8	b	49.0	72.3	295.4	278.2	b
97.0	7.99	296.3	b	49.0	109.3	295.3	415.0	b
97.0	10.8	292.0	b	97.0	120.5	296.3	469.5	b
145.0	8.50	291.8	b					
193.0	3.98	296.4	b					

F) POSITIONS

145. m H_2O 1.1 Torr + CO 3.0 Torr + O_2 4.0 Torr
2.4 m C_2H_2 6.0 Torr

a) the path of the second cell was 25 m with a few Torr of water.
b) the path of the second cell was 2.4 m with 6 Torr of acetylene.

Table 3. Intensity Standards for the Visible Wavelengths based on Measured Water Lines†

POSITIONS in cm^{-1} from Mandin et al. (36)	AVERAGED INTENSITY with uncertainty (rms %)	(OBSERVED - AVERAGED / AVERAGED IN PERCENT) Wilkerson et al. (37) Grating	Mandin et al. (36) FTS	Grossmann Browell (38) TDL	Singh O'Brien (39) ICLS	Unpublished Toth/Brown data FTS
13818.4083	35.6 (± 4.1 %)	1.8%	-5.5%	6.8%	-4.9%	-0.7%
13819.0491	5.33 (± 3.6 %)	-4.3%	-3.6%	5.3%	-1.0%	0.5%
13889.1873	5.82 (± 3.6 %)	-2.0%	-4.8%	2.4%	2.8%	-1.2%
13899.6045	4.20 (± 2.8 %)	-0.7%	-4.5%	2.8%	2.9%	-1.1%
13900.7803	6.75 (± 3.7 %)	0.6%	-5.5%	-0.1%	3.8%	-1.2%
13931.2178	5.44 (± 3.0 %)	-0.8%	-4.5%	2.4%	1.9%	-1.2%
13931.5358	2.87 (± 4.2 %)	-6.6%	-3.0%	3.5%	4.8%	1.4%
Mean difference		-2.0%	-4.5%	3.3%	1.5%	-0.7%
Stand. Dev. (±)		2.4%	0.9%	2.1%	3.1%	1.0%

†The intensities are in 10^{-24} $cm^{-1}/(cm^{-2}\cdot molecule)$ at room temperature. "FTS" in both Mandin et al. and Toth / Brown (unpublished) was the McMath Fourier transform spectrometer at Kitt Peak.

Table 4. Check of the FTS Performance by Remeasuring Water Intensities †

OBSERVED POSITIONS cm^{-1}	OBSERVED MINUS "STANDARD"	OBSERVED INTENSITY	(OBS - STD) / "STANDARD"
13818.4075 (4)	- 0.0009	35.5 (± 1.8 %)	- 0.2 %
13819.0473 (4)	- 0.0018	5.34 (± 1.7 %)	0.4 %
13889.1856 (3)	- 0.0017	5.82 (± 0.7 %)	1.1 %
13899.6043 (3)	- 0.0002	4.34 (± 0.3 %)	3.3 %
13900.7704 (3)	- 0.0009	6.85 (± 0.6 %)	1.5 %
13931.2162 (4)	- 0.0017	5.37 (± 1.1 %)	- 1.3 %
13931.5353 (5)	- 0.0005	2.92 (± 0.9 %)	1.8 %
Mean difference	- 0.0011		+ 0.9 %
Standard Deviation	± 0.0006		± 1.4%

† The experimental uncertainties are shown in parentheses.
The intensities are in units of 10^{-24} $cm^{-1}/(cm^{-2} \cdot molecule)$ at 296 K.
The "standard" positions from Mandin et al. (36) were given with accuracies of ± 0.002 cm^{-1}.
The "standard" intensities are the averaged values from different sources (36-39) in Table 3.

Table 5 Ratio of measured oxygen A-band intensities to 1996 HITRAN values

Type of gas sample†		Present observed / HITRAN
pure oxygen	(Set A)	0.997 (1.0%)
mixed oxygen + nitrogen	(set B)	0.986 (0.8%)
Moist ambient air	(set D)	1.006 (0.7%)
Dry air (cylinder)		0.895 (1.3%)

† The oxygen abundance is assumed to be 20.95 % for both air samples.

Table 6 Measured Line Parameters of the Oxygen A-Band at 13122 cm^{-1}

Positions †	Intensity x 10^{-5}	Upper J	Half Widths N_2 -	Half Widths Self-	Pressure-induced Frequency Shifts N_2 -	Pressure-induced Frequency Shifts Self-	Pressure-induced Frequency Shifts Average ‡	Assignment ΔN NΔJ J
13118.04555	7.711 (1.6)	0	0.0593 (1.5)	0.0588 (1.6)	-0.0025 (2)	-0.0032 (6)	-0.0028	P 1 P 1
13126.39346	3.838 (1.6)	2	0.0609 (3.1)	0.0599 (2.0)	-0.0021 (16)	-0.0033(19)	-0.0027	R 1 R 1
13128.26932	8.951 (1.3)	2	0.0569 (2.5)	0.0561 (2.2)	-0.0020 (6)	-0.0025 (5)	-0.0023	R 1 Q 2
13114.10087	9.661 (1.3)	2	0.0563 (2.2)	0.0551 (1.6)	-0.0039 (2)	-0.0040 (7)	-0.0040	P 3 Q 2
13112.01639	14.27 (0.6)	2	0.0547 (1.6)	0.0539 (1.4)	-0.0043 (4)	-0.0042 (5)	-0.0043	P 3 P 3
13131.49186	10.75 (1.1)	4	0.0546 (0.7)	0.0538 (1.0)	-0.0017 (3)	-0.0026 (5)	-0.0022	R 3 R 3
13133.44172	15.55 (0.8)	4	0.0539 (0.8)	0.0529 (0.5)	-0.0029 (4)	-0.0034 (4)	-0.0032	R 3 Q 4
13107.62884	14.95 (0.2)	4	0.0536 (0.7)	0.0525 (1.6)	-0.0047 (2)	-0.0044 (7)	-0.0046	P 5 Q 4
13105.61746	18.92 (0.8)	4	0.0526 (1.2)	0.0516 (0.7)	-0.0051 (3)	-0.0047 (8)	-0.0049	P 5 P 5
13136.21715	15.76 (1.0)	6	0.0512 (0.9)	0.0505 (1.8)	-0.0025 (4)	-0.0031 (7)	-0.0028	R 5 R 5
13138.20517	20.07 (1.0)	6	0.0512 (1.5)	0.0502 (0.7)	-0.0035 (5)	-0.0035 (3)	-0.0035	R 5 Q 6
13100.82204	17.77 (0.6)	6	0.0511 (1.1)	0.0499 (1.3)	-0.0052 (2)	-0.0046 (3)	-0.0049	P 7 Q 6
13098.84907	21.10 (0.9)	6	0.0509 (0.3)	0.0499 (1.0)	-0.0064 (6)	-0.0058 (3)	-0.0061	P 7 P 7
13140.56811	18.33 (0.6)	8	0.0490 (0.9)	0.0484 (0.8)	-0.0043 (3)	-0.0044 (3)	-0.0044	R 7 R 7
13142.58405	21.99 (0.6)	8	0.0489 (0.9)	0.0484 (0.9)	-0.0046 (2)	-0.0048 (3)	-0.0047	R 7 Q 8
13093.65678	18.22 (0.8)	8	0.0497 (1.5)	0.0483 (1.0)	-0.0063 (4)	-0.0057 (3)	-0.0060	P 9 Q 8
13091.71093	20.77 (0.8)	8	0.0490 (0.8)	0.0484 (1.2)	-0.0059 (2)	-0.0054 (3)	-0.0057	P 9 P 9
13144.54100	18.62 (1.0)	10	0.0474 (1.1)	0.0472 (1.2)	-0.0040 (2)	-0.0042 (4)	-0.0041	R 9 R 9
13146.58038	21.53 (0.7)	10	0.0475 (1.3)	0.0471 (0.8)	-0.0036 (4)	-0.0035 (3)	-0.0036	R 9 Q10
13086.12583	16.73 (0.9)	10	0.0482 (1.9)	0.0473 (1.0)	-0.0061 (2)	-0.0052 (3)	-0.0057	P11 Q10
13084.20390	18.63 (0.9)	10	0.0477 (1.0)	0.0476 (0.9)	-0.0061 (3)	-0.0054 (3)	-0.0058	P11 P11
13148.13604	16.96 (0.8)	12	0.0463 (1.2)	0.0461 (1.5)	-0.0053 (2)	-0.0050 (3)	-0.0052	R11 R11
13150.19683	19.11 (0.9)	12	0.0464 (1.2)	0.0461 (1.6)	-0.0046 (3)	-0.0039 (4)	-0.0043	R11 Q12
13078.22816	13.96 (0.7)	12	0.0466 (0.6)	0.0461 (1.1)	-0.0064 (3)	-0.0057 (3)	-0.0061	P13 Q12
13076.32856	15.33 (1.0)	12	0.0467 (0.8)	0.0460 (1.1)	-0.0070 (4)	-0.0065 (3)	-0.0068	P13 P13

Table 6 (Continued)

Positions	Intensity x 10^{-5}	Upper J	Half Widths N_2 -	Half Widths Self-	Pressure-induced Frequency Shifts N_2 -	Pressure-induced Frequency Shifts Self-	Pressure-induced Frequency Shifts Average ‡	Assignment ΔN NΔJ J
13151.34898	14.13 (1.1)	14	0.0445 (0.8)	0.0450 (1.6)	-0.0052 (3)	-0.0051 (5)	-0.0052	R13 R13
13153.43079	15.62 (0.8)	14	0.0447 (1.5)	0.0447 (1.9)	-0.0049 (2)	-0.0045 (2)	-0.0047	R13 Q14
13069.96200	10.80 (0.6)	14	0.0457 (1.2)	0.0449 (1.6)	-0.0052 (4)	-0.0050 (4)	-0.0051	P15 Q14
13068.08212	11.68 (1.3)	14	0.0445 (1.2)	0.0452 (1.6)	-0.0060 (2)	-0.0054 (3)	-0.0064	P15 P15
13154.17969	10.80 (0.9)	16	0.0435 (2.7)	0.0437 (1.4)	-0.0063 (4)	-0.0061 (5)	-0.0062	R15 R15
13156.28118	11.89 (0.9)	16	0.0436 (0.8)	0.0437 (1.1)	-0.0066 (4)	-0.0053 (3)	-0.0060	R15 Q16
13061.32737	7.633 (1.0)	16	0.0435 (2.6)	0.0439 (1.4)	-0.0058 (4)	-0.0046 (4)	-0.0052	P17 Q16
13059.46714	8.289 (0.9)	16	0.0429 (1.0)	0.0439 (1.5)	-0.0068 (5)	-0.0060 (3)	-0.0064	P17 P17
13156.62279	7.777 (0.8)	18	0.0424 (1.6)	0.0428 (1.6)	-0.0051 (7)	-0.0041 (6)	-0.0046	R17 Q18
13158.74399	8.400 (2.2)	18	0.0408 (1.9)	0.0421 (3.4)	-0.0050 (13)	-0.0051 (7)	-0.0051	R17 R17
13052.32403	5.167 (1.3)	18	0.0417 (1.5)	0.0424 (2.1)	-0.0080 (4)	-0.0066 (8)	-0.0073	P19 Q18
13050.48078	5.494 (1.2)	18	0.0407 (2.4)	0.0423 (2.0)	-0.0059 (6)	-0.0052 (9)	-0.0059	P19 P19
13158.68085	5.270 (1.3)	20	0.0389 (2.1)	0.0421 (3.4)	-0.0074 (18)	-0.0081 (12)	-0.0078	R19 R19
13160.81486	5.591 (1.0)	20	0.0410 (2.9)	0.0416 (2.3)	-0.0082 (17)	-0.0087 (13)	-0.0085	R19 Q20
13042.94893	3.230 (1.4)	20	0.0393 (3.1)	0.0400 (2.7)	-0.0086 (6)	-0.0088 (19)	-0.0085	P21 Q20
13041.12509	3.411 (1.7)	20	0.0402 (3.3)	0.0411 (3.7)	-0.0088 (9)	-0.0071 (16)	-0.0080	P21 P21
13160.33962	3.234 (1.5)	22		0.0411 (2.8)		-0.0080 (20)		R21 R21
13031.39038	1.960 (1.7)	22		0.0392 (2.0)				P23 P23
13033.19668	1.895 (1.8)	22	0.0374 (4.0)	0.0408 (3.4)				P23 Q22

† **Positions in cm^{-1}, intensities in natural abundance in cm^{-2}/atm at 296 K and widths and pressure shifts in cm^{-1}/atm at 296 K .** The value in parentheses is the computed rms of the average in % for widths and in 0.0001 cm^{-1}/atm for the shifts; **these should be taken to be the precision, not the absolute accuracy of the result.**

‡ **The average shift is computed using shifts for N_2 - and self-broadening; it can be used for the air-broadened pressure shift.**

Table 7 **Oxygen A-band: upper state energies and pressure coefficients averaged by J †**

UPPER STATE J' N'	E' (unc) cm^{-1}	rms	PRESSURE-BROADENED WIDTHS N_2- Width	% rms	% o-c	Self- Width	% rms	% o-c	TEMPERATURE DEPENDENCE "n" N_2-	% rms	Self-	% rms	COMPUTED air- Width	air- "n"
0	13122.0067		0.0593		0.6	0.0588		1.2	0.77		0.67		0.0591	0.72
2	13130.3539	(5)	0.0572	(4.6)	1.2	0.0562	(4.6)	+1.0	0.73	(7.8)	0.67	(7.8)	0.0569	0.70
4	13149.8391	(2)	0.0537	(1.5)	0.9	0.0527	(1.7)	-1.1	0.77	(4.5)	0.70	(5.5)	0.0535	0.74
6	13180.4292	(3)	0.0511	(0.3)	1.7	0.0503	(0.7)	-1.8	0.74	(4.4)	0.71	(5.6)	0.0509	0.73
8	13222.1487	(2)	0.0492	(0.8)	-1.4	0.0484	(0.1)	-1.8	0.74	(4.5)	0.74	(2.6)	0.0490	0.74
10	13274.9786	(3)	0.0477	(0.8)	-0.4	0.0473	(0.5)	-0.4	0.72	(4.2)	0.71	(2.6)	0.0475	0.72
12	13338.9108	(5)	0.0465	(0.4)	1.0	0.0461	(0.1)	0.5	0.73	(5.6)	0.71	(2.9)	0.0464	0.72
14	13413.9316	(1)	0.0449	(1.2)	1.3	0.0450	(0.5)	1.3	0.68	(4.1)	0.66	(4.4)	0.0449	0.67
16	13500.0290	(4)	0.0434	(0.7)	1.6	0.0438	(0.4)	1.6	0.65	(3.6)			0.0435	0.65
18	13597.1853	(7)	0.0414	(1.9)	0.5	0.0424	(0.7)	-0.9	0.65	(6.0)			0.0416	0.65
20	13705.3846	(4)	0.0399	(2.3)	0.2	0.0412	(2.2)	0.4	0.60	(19.0)			0.0401	
22	13824.6031	(2)	0.0376	(3.9)	-2.5	0.0406	(1.4)	0.8					0.0382	average=
24	13954.8222	(4)	0.0376	(5.0)	0.5	0.0387	(5.0)	-2.4					0.0378	0.70 (4)

† Upper state energies are determined by adding the calculated ground state (16) to observed individual positions.
For J'=O, the levels and pressure coefficients obtained for P1P1 are listed..
Widths are in units of cm^{-1}/atm at 296 K. "n" is obtained from $\ln [\gamma] = \ln [\gamma_o] + n \ln [T_o / T]$ where T_o = 296 K.
The observed - calculated columns are computed using the following expressions for the widths with J = J'
Fitted nitrogen- broadened width = $0.05896 - 0.001253\ J + 0.000014797\ J^2$; the % rms of O-C (observed - computed) is 1.1%
Fitted self-broadened width = $0.05810 - 0.001268\ J + 0.000020829\ J^2$; the % rms of O-C (observed - computed) is 1.2%
Air- widths are computed assuming a mixture of "clean dry air" with 79% nitrogen and 21.% oxygen.
"Air-n", the temperature dependence coefficient for the widths for air, is the average of the self- and nitrogen- values for "n".

Table 8 Comparison of line positions for the oxygen A-band †

	Reference	Positions in cm^{-1} Present - other	Rms
(13)	Schermaul and Learner	0.0015	± 0.0007
(51)	Kanamori et al.	0.003	± 0.007
(52)	Phillips et al.	0.012	± 0.0005
(16)	1996 HITRAN	0.0128 --> 0.0046 (J'=0 --> J'=20)	

Table 9 Comparison of pressure-induced frequency shifts in the oxygen A-band †

	Reference	Self	Nitrogen
		FOR TRANSITIONS RANGING FROM J' = 0 TO Jmax ‡	
	Present	- 0.0025 --> - 0.0087	- 0.0020 --> - 0.0088
(54)	Phillips & Hamilton	- 0.0069 --> - 0.0168	- 0.0160 --> - 0.0208
		INDIVIDUAL TRANSITIONS	
		R15Q16	R17R17
	Present	- 0.0053 (3)	- 0.0051 (7)
(7)	Avetisov & Kauranen	- 0.0058 (10)	- 0.0061 (15)

† Pressure-induced frequency shifts are in units of cm^{-1} / atm at room temperature.
‡ Jmax is 22 for the present study and 16 for Ref. 54.

Table 10 Estimated experimental precisions and absolute accuracies

Oxygen A-band Parameter †	Precision	Accuracy
Line position	0.00035	0.0015
Pressure-induced frequency shift	0.0006	0.0015
Line intensity	1.0%	2.0%
Lorentz width (HWHM)	1.2%	2.5%
Width temperature dependence	6 %	15 %
Shifts temperature dependence	Not reported	

† positions are in cm^{-1}, and shifts are in cm^{-1}/atm.

List of figure captions

Fig. 1. The absorption spectrum of the oxygen A-band at 13122 cm^{-1} (760 nanm. 0.76 μm) recorded at 0.02 cm^{-1} resolution using the McMath Fourier transform spectrometer at the National Solar Observatory located at Kitt Peak. The path is 2.4 m, and the pressure is 388.4. Torr at 297.1 K.

Fig. 2. Measurement of line position, intensity and widths through non-linear least square curve fitting. The differences between the observed and synthetic spectra are minimized by adjusting the parameters in the computed spectrum until the residuals are dominated by the signal to noise. The path is 2.4 m, and the pressure is 441. Torr at 297.2 K.

Fig. 3. Comparison of 1996 HITRAN calculated values to the present intensities.

Fig. 4. The measured self-broadened widths (HWHM) of the oxygen A-band vs the upper state quantum number N = J.

Fig. 5. The measured nitrogen-broadened widths (HWHM) of the oxygen A-band vs the upper state quantum number N = J.

Fig. 6. Comparison of the self- broadened widths of the oxygen A-band: The ratio is the J-averaged widths of others divided by the corresponding present values from Table 7. The plot symbols are 1) Ritter and Wilkerson (12) and 2) Schermaul et al. (13).

Fig. 7. The measured self-broadened pressure-induced frequency shifts of the oxygen A-band vs the upper state quantum number N = J.

Fig. 8. The measured nitrogen-broadened pressure-induced frequency shifts of the oxygen A-band vs the upper state quantum number N = J.

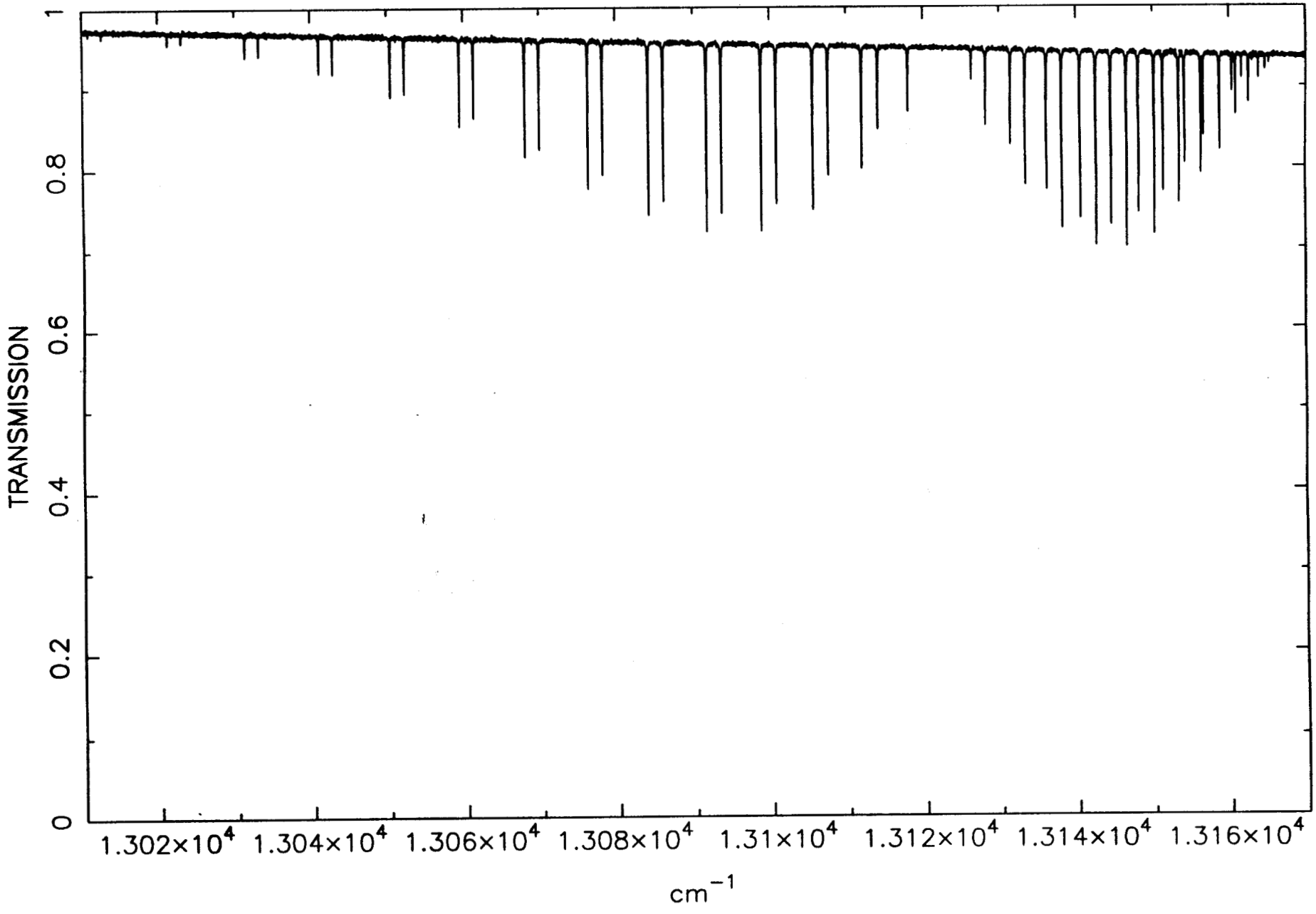

run: j136.29 date: 10/24/97 resolution: 0.020385 linefile: NONE

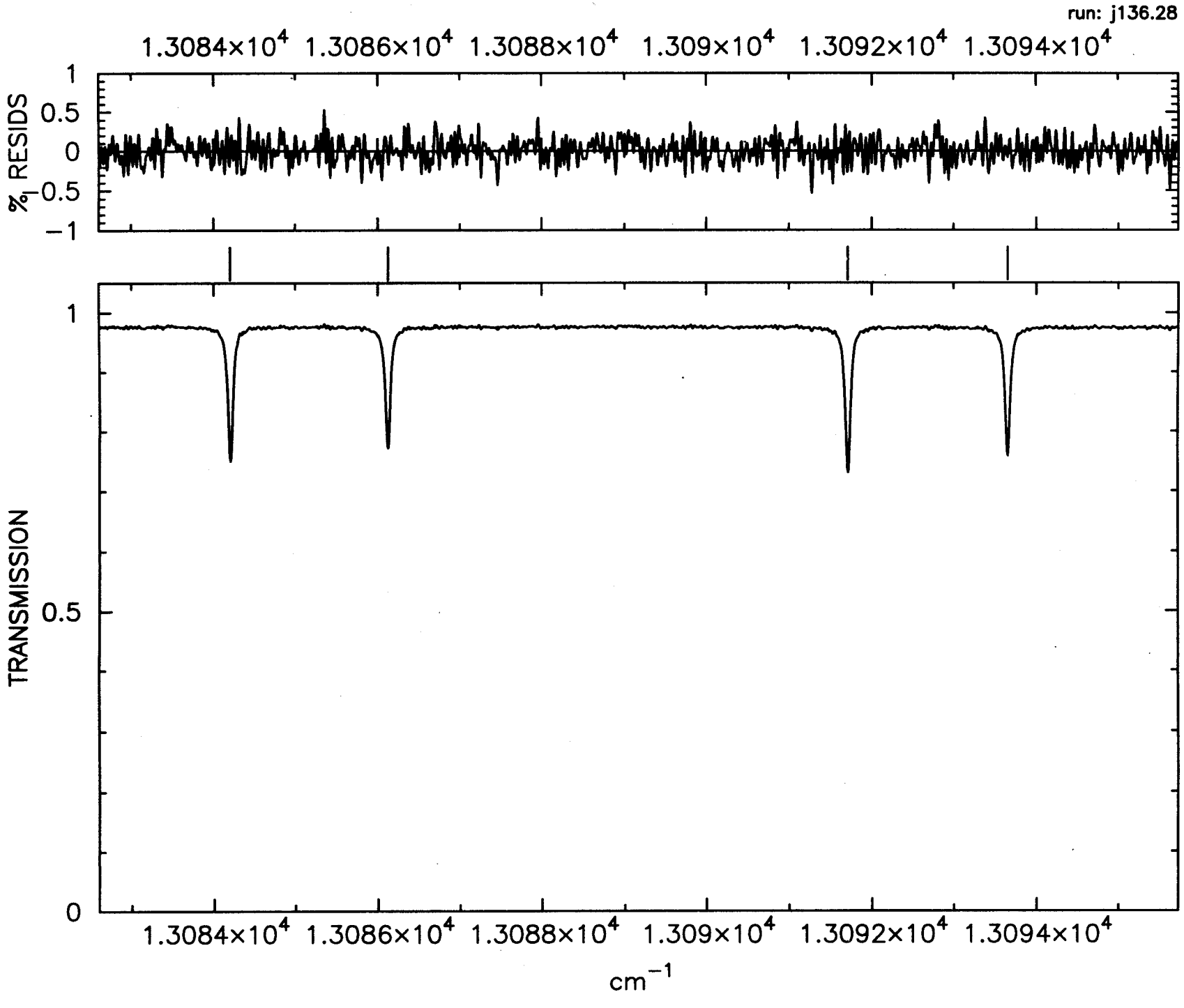
run: j136.28
1.3084×10^4 1.3086×10^4 1.3088×10^4 1.309×10^4 1.3092×10^4 1.3094×10^4
1
0.5
0
−0.5
−1
%_I RESIDS
1
0.5
0
TRANSMISSION
1.3084×10^4 1.3086×10^4 1.3088×10^4 1.309×10^4 1.3092×10^4 1.3094×10^4
cm^−1

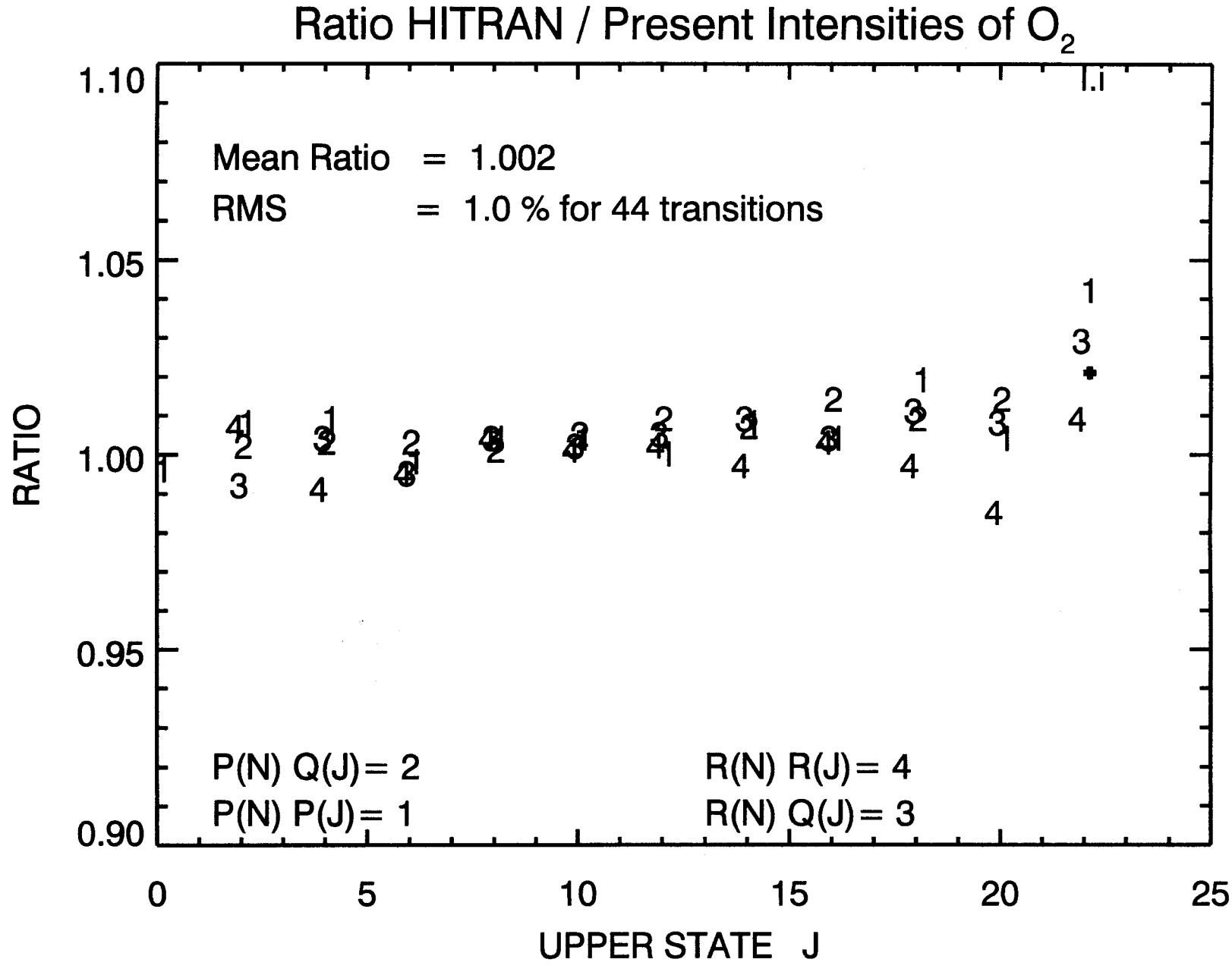
Ratio HITRAN / Present Intensities of O_2
Mean Ratio = 1.002
RMS = 1.0 % for 44 transitions
P(N) Q(J)= 2
P(N) P(J)= 1
R(N) R(J)= 4
R(N) Q(J)= 3
RATIO
UPPER STATE J
1.10
1.05
1.00
0.95
0.90
0
5
10
15
20
25

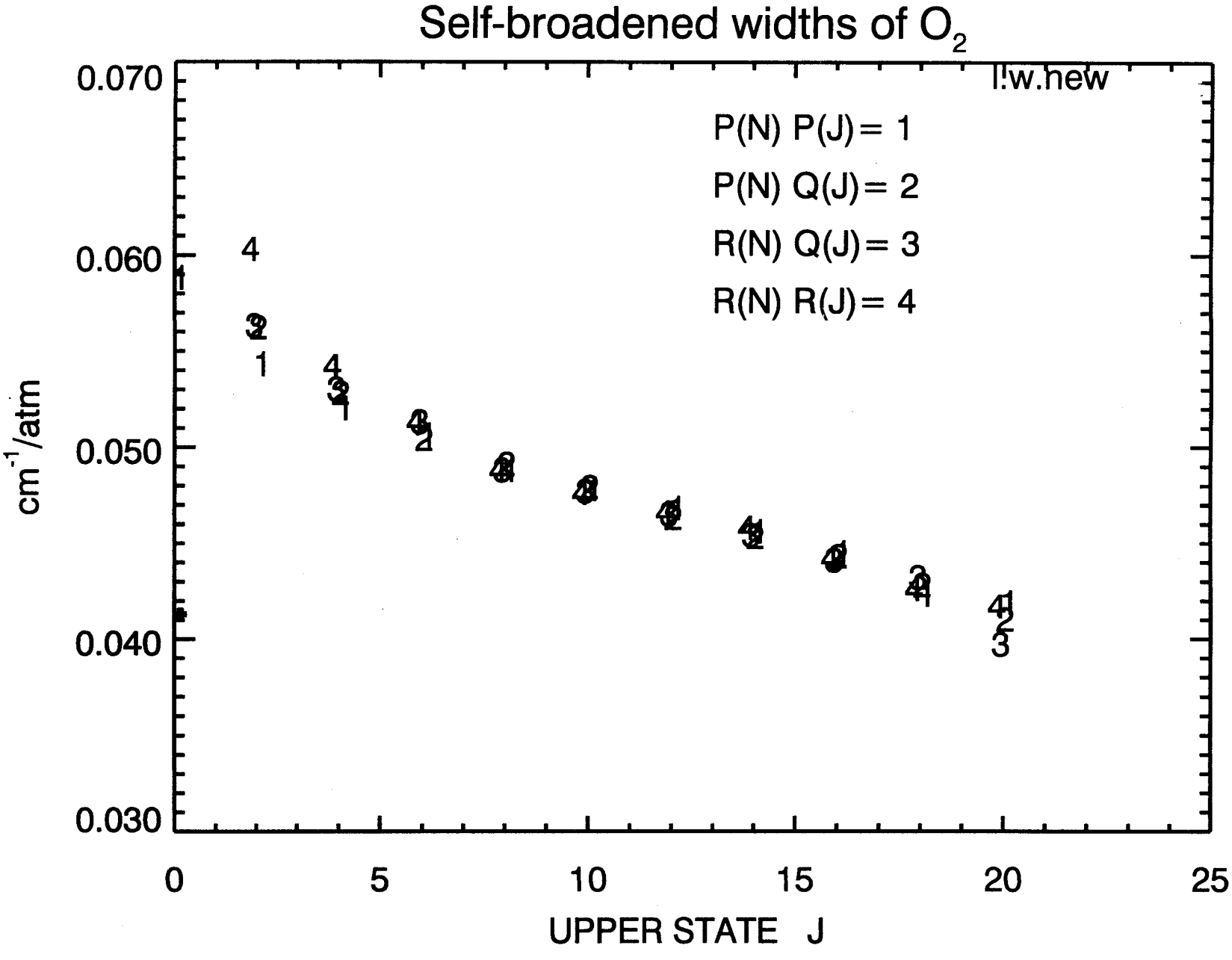
Self-broadened widths of O_2
l!w.new
P(N) P(J)= 1
P(N) Q(J)= 2
R(N) Q(J)= 3
R(N) R(J)= 4
0.070
0.060
0.050
0.040
0.030
cm^{-1}/atm
0
5
10
15
20
25
UPPER STATE J

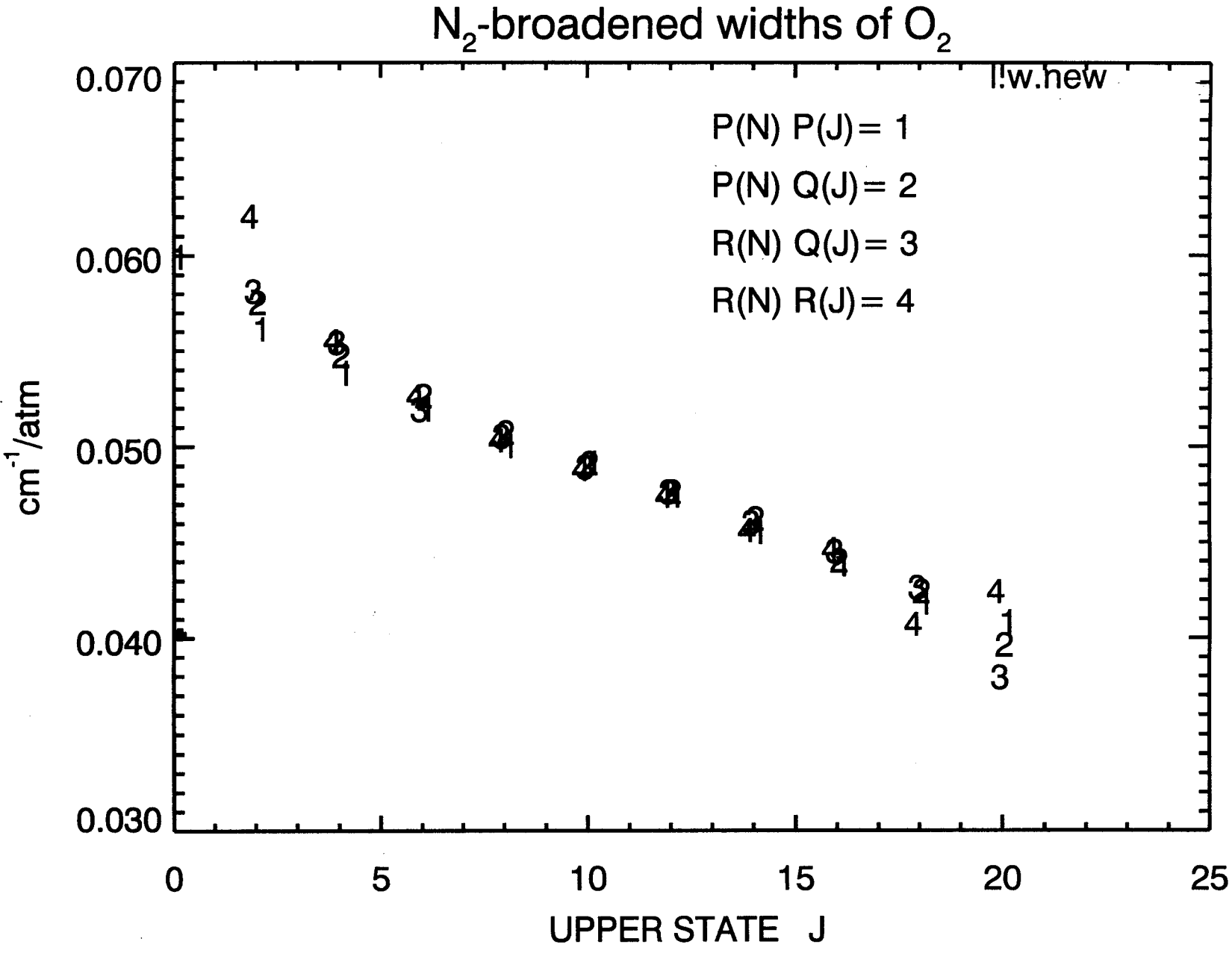
N2-broadened widths of O2
!w.new
P(N) P(J)= 1
P(N) Q(J)= 2
R(N) Q(J)= 3
R(N) R(J)= 4
0.070
0.060
0.050
0.040
0.030
cm-1/atm
0
5
10
15
20
25
UPPER STATE J

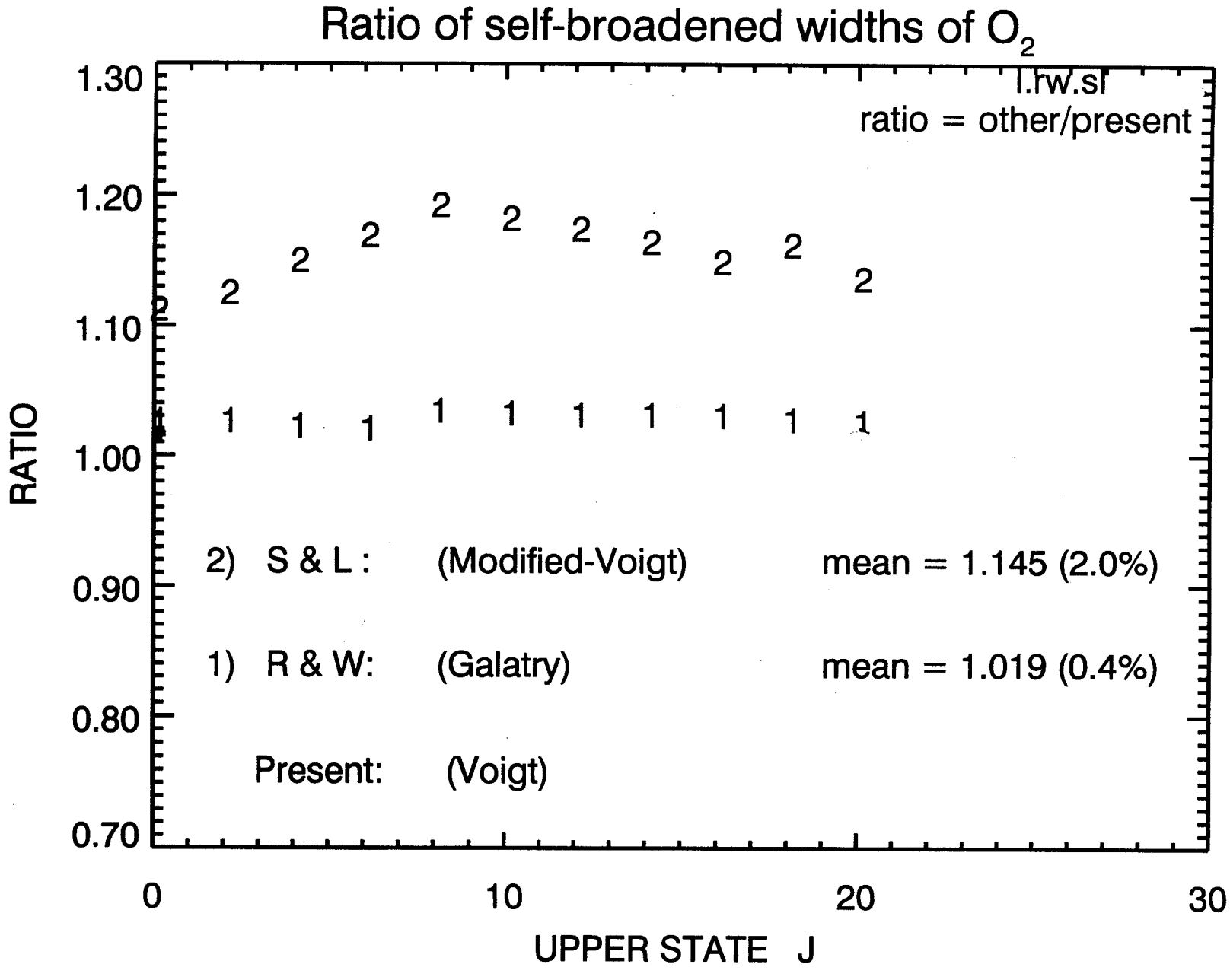
Ratio of self-broadened widths of O_2
l.rw.sl
ratio = other/present
1.30
1.20
1.10
1.00
0.90
0.80
0.70
RATIO
2 2 2 2 2 2 2 2 2
1 1 1 1 1 1 1 1 1
2) S & L : (Modified-Voigt) mean = 1.145 (2.0%)
1) R & W: (Galatry) mean = 1.019 (0.4%)
Present: (Voigt)
0
10
20
30
UPPER STATE J

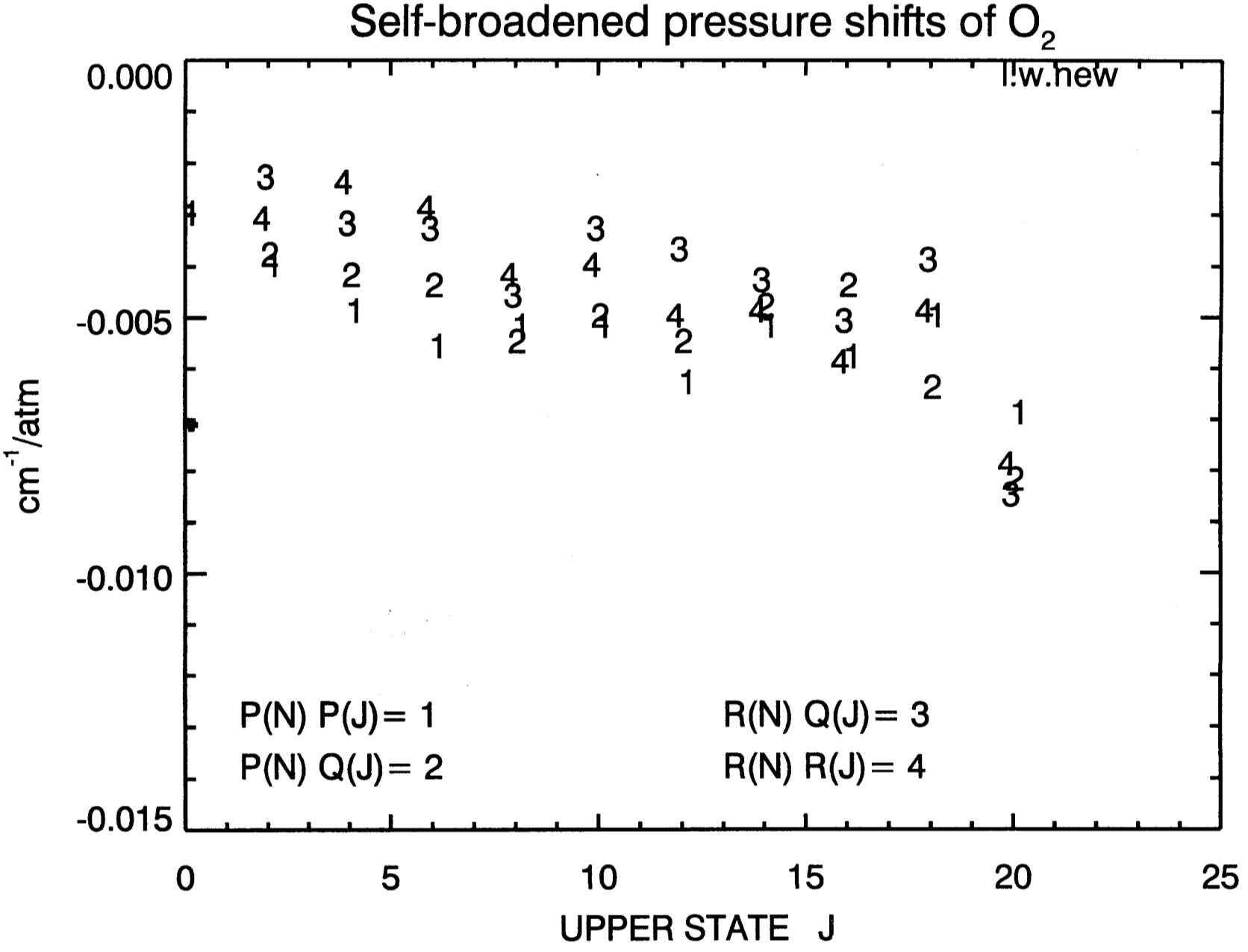
Self-broadened pressure shifts of O_2
!w.new
0.000
-0.005
-0.010
-0.015
cm^{-1}/atm
P(N) P(J)= 1
P(N) Q(J)= 2
R(N) Q(J)= 3
R(N) R(J)= 4
0
5
10
15
20
25
UPPER STATE J

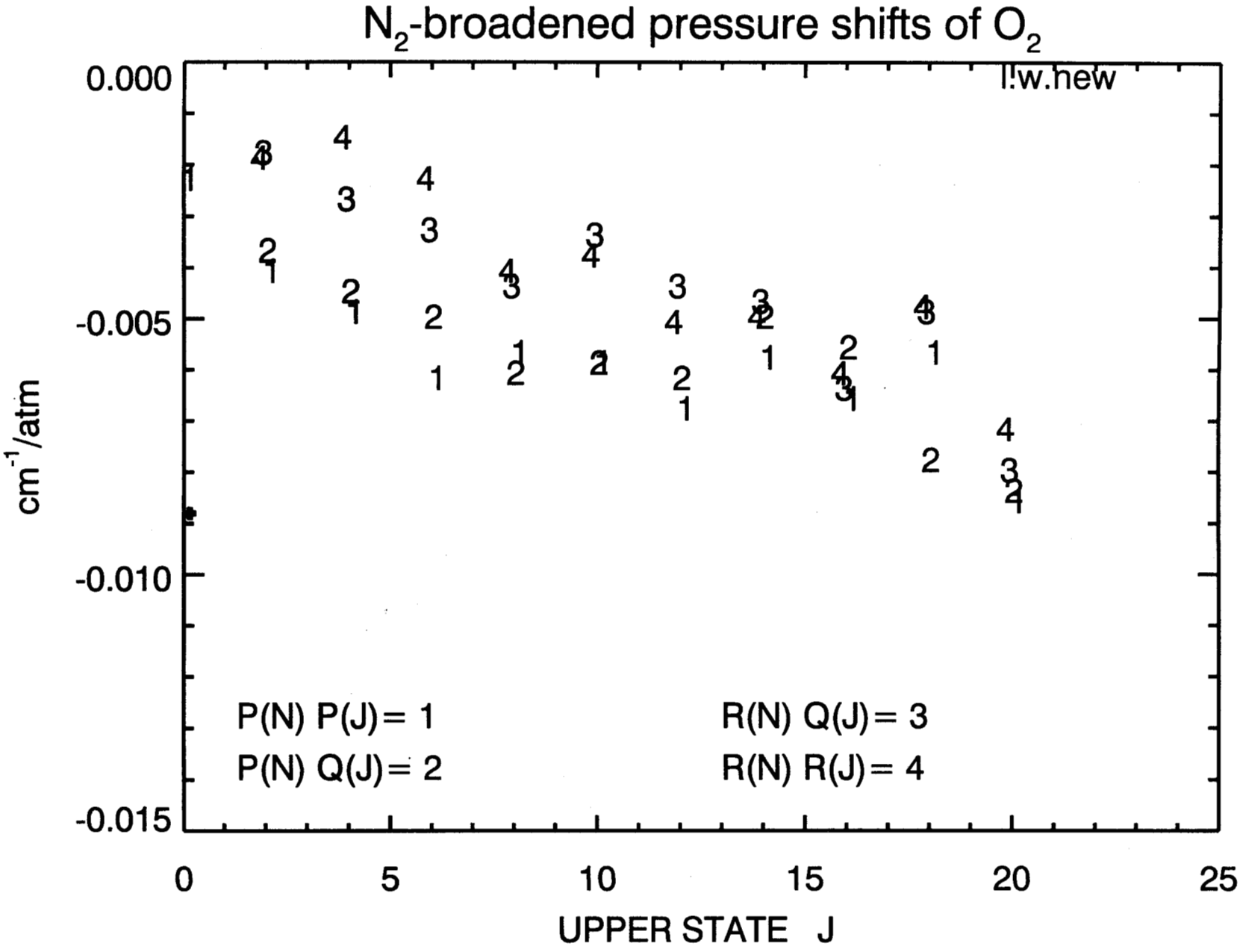
N2-broadened pressure shifts of O2
lw.new
0.000
-0.005
-0.010
-0.015
cm-1/atm
P(N) P(J)= 1
P(N) Q(J)= 2
R(N) Q(J)= 3
R(N) R(J)= 4
0
5
10
15
20
25
UPPER STATE J